EurJOC
European Journal of Organic Chemistry

Chemistry Europe
European Chemical Societies Publishing

Accepted Article

Title: An Efficient Cyclic Di-AMP Based Artificial Metalloribozyme for Enantioselective Diels–Alder Reactions

Authors: Qianqian Qi, Shuting Lv, Min Hao, Xingchen Dong, Youkun Gu, Peizhe Wu, Wenyue Zhang, Yashao Chen, and Changhao Wang

To be cited as: *Eur. J. Org. Chem.* 10.1002/ejoc.202000652

Link to VoR: https://doi.org/10.1002/ejoc.202000652

WILEY-VCH

10.1002/ejoc.202000652

WILEY-VCH

An Efficient Cyclic Di-AMP Based Artificial Metalloribozyme for Enantioselective Diels–Alder Reactions

Qianqian Qi, Shuting Lv, Min Hao, Xingchen Dong, Youkun Gu, Peizhe Wu, Wenyue Zhang, Yashao Chen,* and Changhao Wang*[a]

[a] Q. Qi, S. Lv, M. Hao, Y. Gu, P. Wu, W. Zhang, Prof. Y. S. Chen, Dr. C. Wang
Key Laboratory of Applied Surface and Colloid Chemistry, Ministry of Education
School of Chemistry and Chemical Engineering, Shaanxi Normal University,
620 West Chang'an Avenue, 710119 Xi'an, China
E-mail: changhaowang@snnu.edu.cn
yschen@snnu.edu.cn

Supporting information for this article is given via a link at the end of the document.

Abstract: The diverse structures of nucleic acids as scaffolds have brought the significant advancement for DNA-based enantioselective catalysis, yet RNA-based enantioselective catalysis is lack of investigation. Herein, we report that a small, natural RNA of cyclic di-AMP (c-di-AMP) and Cu^{2+} ions assemble into an artificial metalloribozyme (c-di-AMP·Cu^{2+}) that could effectively catalyze the enantioselective Diels–Alder reactions with up to 80% *ee*. The enantioselective catalytic performance of c-di-AMP·Cu^{2+} has been studied by thorough investigations of different metal cofactors, c-di-AMP/Cu^{2+} molar ratios, additives, buffers and c-di-AMP analogues. In addition, the assembly of c-di-AMP·Cu^{2+} gives rise to a 300-fold and 5-fold rate acceleration compared to the uncatalyzed reaction and Cu^{2+} ions, respectively. This work provides a simple and efficient strategy to construct the RNA-based catalysts that would expand the current nucleic acids-based catalysis and might hint the possible catalytic RNA in primordial chemistry.

Introduction

In recent years, the natural chiral structures of nucleic acids have attracted much attention of chemists to construct nucleic acid-based hybrid catalysts for enantioselective catalysis. In 2005, Roelfes and Feringa reported the first DNA-based hybrid catalyst composing of double-stranded DNA (dsDNA) and achiral copper(II) complex that could modestly achieved an enantioselective Diels–Alder (D–A) reaction.[1] This concept of dsDNA-based asymmetric catalysis has been applied to several Lewis acid catalysis[2] and organometallic catalysis[3] in aqueous media. Recently, G-quadruplex DNA (G4DNA) that specifically binds to metal ions or complexes has been reported to achieve several enantioselective transformations.[4] Moreover, the enantioselectivities of the G4DNA-based catalysis are largely dependent on the tunable features of the G-quadruplex structures.[4b, 4d, 5] In addition, G-triplex DNA,[6] artificial deoxyribozyme,[7] unnatural DNA[8] and guanosine-based assembly[9] were also employed as scaffolds to construct nucleic acid-based hybrid catalysts.

Compared to DNA, very few examples of RNA-based enantioselective catalysis were reported owing to its comparably lower stability. In 2000, Jäschke and coworkers reported that a synthetic 49-mer ribozyme could catalyze an enantioselective Diels–Alder reaction between anthracene and maleimide with an enantiomeric excess (*ee*) value over 90%.[10] Arseniyadis and co-workers have recently designed an unnatural double-stranded RNA-based hybrid catalyst for a Friedel–Crafts reaction with modest enantioselectivity.[11] Marek and Hennecke demonstrated that DNA is a more effective scaffold than RNA to recognize metal complexes to assemble into nuclei acid based hybrid catalysts.[12] Very recently, our group has reported that an artificial metalloribozyme of a cyclic dinucleotide termed cyclic di-AMP (c-di-AMP) and copper(II) ions that could high-efficiently catalyze enantioselective Friedel–Crafts reactions with up to 97% *ee* and the structure of the artificial metalloribozyme was proposed in a dimer form.[13]

Cyclic dinucleotides (CDNs) are natural cyclic RNA molecules of that serve as important second messengers and regulate many cellular processes.[14] So far, five CDNs of c-di-GMP, c-di-AMP, c-AMP-GMP, 2'3'-cGAMP and c-AMP-UMP have been discovered in nature.[15] The CDNs have been identified to form stable tertiary structures as evidenced by theoretical calculations and experimental studies,[16] making them as promising scaffolds to construct CDN-based hybrid catalysts. In this work, we report that c-di-AMP and copper(II) ions are assembling into an artificial metalloribozyme (c-di-AMP·Cu^{2+}) that could efficiently catalyze the enantioselective D–A reactions (Scheme 1).

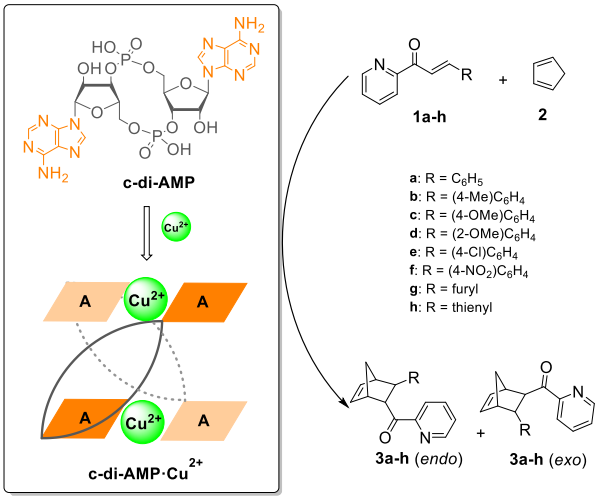

Scheme 1. Schematic representation of enantioselective Diels–Alder reactions between aza-chalcones (**1a-h**) and cyclopentadiene (**2**) catalyzed by a c-di-AMP based artificial metalloribozyme (c-di-AMP·Cu^{2+}).

Results and Discussion

The catalytic performance of c-di-AMP based metallo-RNA with different metal cofactors

We selected an enantioselective D–A reaction of aza-chalcone (**1a**) and cyclopentadiene (**2**) as a benchmark reaction to examine the catalytic properties of c-di-AMP based metallo-RNA. C-di-AMP has been demonstrated to fold into highly ordered structure as evidenced by the circular dichroism (CD) spectrum (Figure S1). Of note, the folded c-di-AMP alone slightly promotes the D–A reaction to provide a conversion of 13%, an *endo*/*exo* of 92:8 and an enantioselectivity of 18% *ee* (Table 1, entry 1). These results suggest that c-di-AMP in a tertiary scaffold shows weak activity to yield the chiral product which is similar as G4DNA based catalysis[4b, 4c] and c-di-AMP catalyzed Friedel-Crafts reaction.[13] Once the copper(II) nitrate was added to c-di-AMP, the conversion of the corresponding D–A reaction remarkably improves to nearly 90% and the enantioselectivity increases to 61% *ee* (Table 1, entry 2), indicating that copper(II) ions are effectively interacting with c-di-AMP to assemble into a c-di-AMP based artificial metalloribozyme (c-di-AMP·Cu^{2+}). When altering different copper(II) salts as metal cofactors, the corresponding D–A reactions show insignificant changes of the *endo*/*exo* and the *ee* values (Table 1, entries 2-5) and the c-di-AMP·Cu^{2+} using $Cu(OTf)_2$ as metal cofactor provides an excellent conversion of 98% and 65% *ee* (Table 1, entry 5). In addition, the CD spectra display the similar profiles of c-di-AMP in the presence of copper(II) salts with different anions (Figure S2a). These results indicate that the Cu^{2+} ions are efficient metal cofactors to assist c-di-AMP to exert the enantioselective catalytic performance and the c-di-AMP·Cu^{2+} shows an independent behavior with the counter-anions of copper(II) salts.

Furthermore, different copper(II) complexes were investigated as metal cofactors for the c-di-AMP based artificial metalloribozyme. Four achiral ligands of bipyridine (bpy), 4,4'-dimethylbipyridine (dmbpy), phenanthroline (phen) and terpyridine (tpy) were employed to coordinate with copper(II) nitrate to form the complexes. Compared to Cu^{2+} ions as cofactors, the introduction of achiral ligand to c-di-AMP·Cu^{2+} yields the reduced conversion, diastereoselectivity and enantioselectivity to the corresponding D–A reactions (Table 1, entries 6-9). Considering the chiral structures, the CD spectra of c-di-AMP with different copper(II) complexes show the similar typical peaks but varied intensity compared to c-di-AMP·Cu^{2+} (Figure S2b). The above results show that the extra ligand causes negative effect to c-di-AMP·Cu^{2+} catalyzed D–A reaction that is similar as previously reported.[13] The reduction of the enantioselectivities might be ascribed to the presence of ligand that causes the perturbation of the chiral microenvironment and the hindrance between aza-chalcone substrate and Cu^{2+} ions.

In short, the above data demonstrate that Cu^{2+} ions are specifically binding to c-di-AMP to form a potent metalloribozyme. From the recent report of c-di-AMP·$Cu^{2+}$of the catalyzed Friedel-Crafts reaction,[13] the structure of c-di-AMP·Cu^{2+} is depicted in a dimeric form where two c-di-AMP are stacking intercrossingly and the Cu^{2+} ions are sitting in the center of an adenine-adenine plane (Scheme 1). For the binding affinity of Cu^{2+} ions in adenine-containing nucleotides/nucleosides, the N7 atom in the purine moiety and the phosphates have been proved as the preferred binding sites.[17] The coordination structures of N7-Cu^{2+} and P(O)-Cu^{2+} would yield a macro-chelate formation.[18] Based on the structure of c-di-AMP, the highly specific bonding of Cu^{2+} ions is possibly ascribed to the presence of two N7 atoms and the phosphate groups in the c-di-AMP dimer.

Table 1. Enantioselective Diels–Alder reaction catalyzed by c-di-AMP in the presence of different metal cofactors.[a]

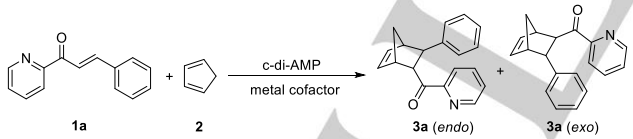

Entry	Metal cofactor	Conv. (%)	*endo*/*exo*	*ee* (**3a**%, *endo*)
1	none	13	92:8	18
2	$Cu(NO_3)_2$	89	94:6	61
3	$CuSO_4$	85	92:8	64
4	$CuCl_2$	80	94:6	65
5	$Cu(OTf)_2$	98	93:7	65
6	Cu(bpy)	67	89:11	37
7	Cu(dmbpy)	69	87:13	40
8	Cu(phen)	57	91:9	55
9	Cu(tpy)	56	91:9	49

[a] Reaction conditions: **1a** (2 μmol), **2** (250 μmol), c-di-AMP (250 μM), metal cofactor (50 μM), MES buffer (500 μL, 20 mM, pH 5.5), 4 °C, 24 h. Achiral ligands: bpy, bipyridine; dmbpy, 4,4'-dimethylbipyridine; phen, phenanthroline; tpy, terpyridine.

The molar ratio effect of c-di-AMP and Cu^{2+}

For the assembly of c-di-AMP·Cu^{2+}, c-di-AMP mainly contributes

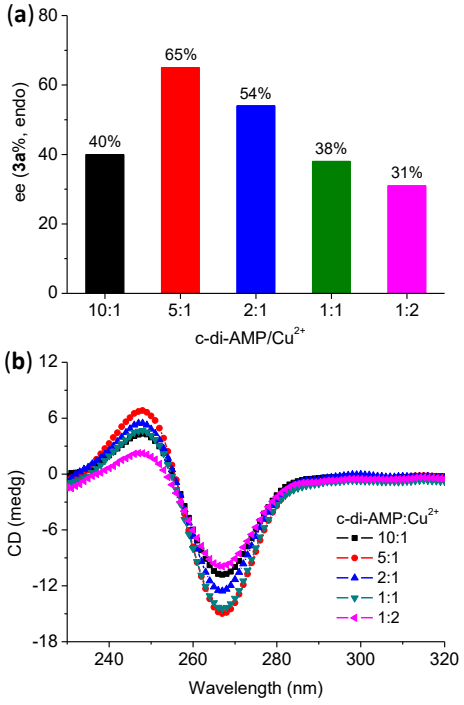

Figure 1. (a) The *ee* of **3a** (*endo*) that was produced by c-di-AMP·Cu^{2+} catalyzed Diels-Alder reactions with different molar ratios. Reaction conditions: **1a** (1 μmol), **2** (250 μmol), c-di-AMP (250 μM), $Cu(OTf)_2$ (25-500 μM), MES buffer (500 μL, 20 mM, pH 5.5), 4 °C, 24 h. (b) CD spectra of c-di-AMP (250 μM) in the presence of $Cu(OTf)_2$ at different concentrations (25-500 μM).

to the chiral induction and the Cu^{2+} ions are the catalytic species. Therefore, the molar ratio between c-di-AMP and Cu^{2+} ions is a key factor to determine the enantioselective activity of c-di-AMP·Cu^{2+}. We investigated different molar ratios of c-di-AMP/Cu^{2+} with a fixed concentration of c-di-AMP at 250 μM. Compared to the c-di-AMP promoted benchmark reaction (Table 1, entry 1), the addition of a small amount of Cu^{2+} ions (25 μM) could increase the conversion from 13% to 83% and enhance the *ee* from 18% to 40% with c-di-AMP/Cu^{2+} = 10:1 (Figure 1a, Table S1). When the molar ratio of c-di-AMP/Cu^{2+} is at 5:1, the corresponding D–A reaction provides an approximately full conversion and an enhanced *ee* of 65% (Figure 2). Further increasing the molar ratios of c-di-AMP/Cu^{2+}, the conversions of the corresponding D–A reactions show no significant changes (Table S1) yet the *ee* values of **3a** are gradually decreasing (Figure 1a). These results indicate that the coordination between c-di-AMP and Cu^{2+} ions is feasible at the molar ratio of 5:1. Continue increasing the amount of Cu^{2+} ions will enhance the racemic reaction, thus resulting in a decreased *ee* value. Furthermore, the chiral structures of c-di-AMP/Cu^{2+} with various molar ratios were characterized. Although c-di-AMP/Cu^{2+} with different molar ratios display the similar CD profiles, the intensity of c-di-AMP/Cu^{2+} at 5:1 is the highest (Figure 1b), indicating that c-di-AMP/Cu^{2+} at 5:1 forms a more compact structure. Taken together, the molar ratio of c-di-AMP/Cu^{2+} causes great effect to c-di-AMP·Cu^{2+} catalyzed D-A reaction and the c-di-AMP/Cu^{2+} at 5:1 exhibits the best catalytic performance.

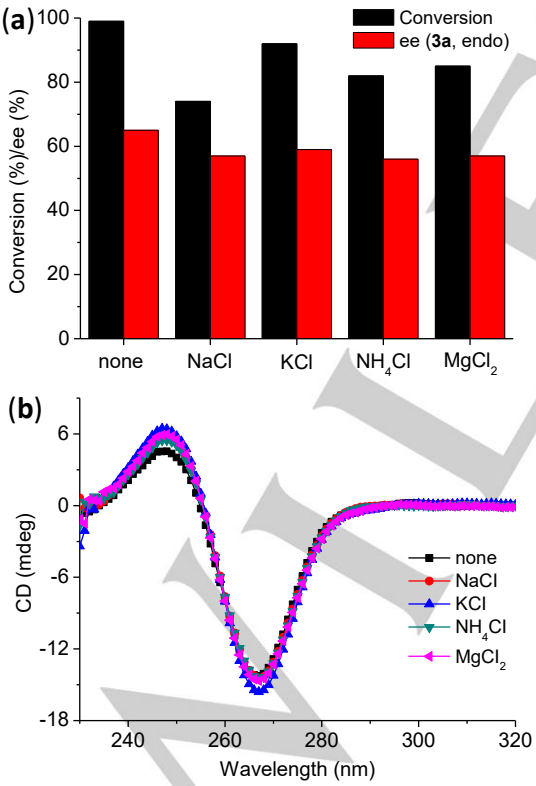

Figure 2. (a) c-di-AMP·Cu^{2+} catalyzed Diels–Alder reaction with different additives at 10 mM and (b) the corresponding CD spectra. Reaction conditions: **1a** (2 μmol), **2** (250 μmol), c-di-AMP (250 μM), $Cu(OTf)_2$ (50 μM), additive (MCl or MCl_2, 10 mM), MES buffer (500 μL, 20 mM, pH 5.5), 4 °C, 24 h.

The effect of additives

In nature, the structures of nucleic acids are sensitive to the presence of additive metal ions such as alkaline metal ions (Na^+, K^+) and alkaline earth metal ions (Mg^{2+}). Furthermore, the presence of Na^+ or K^+ has been demonstrated to cause great effect in G4DNA-based enantioselective catalysis.[5] Compared to c-di-AMP·Cu^{2+} catalyzed benchmark D–A reaction without additive metal ions, the addition of 10 mM Na^+, K^+ or Mg^{2+} causes negligible effect to the corresponding enantioselectivities yet results in slight decrement of the conversions (Figure 2a). These results indicate that the tertiary structure of c-di-AMP is independent on the additional metal ion which is different from the G-quadruplex structures. In addition, the presence of ammonium ions (NH_4^+) shows the similar effect as the above metal ions (Figure 2a). Compared to the c-di-AMP·Cu^{2+} without any additive, the corresponding CD spectra of c-di-AMP·Cu^{2+} with different additives show the similar representative peaks and the intensities (Figure 2b), suggesting that the additives cause negligible effect to the chiral structure of c-di-AMP·Cu^{2+}. This might be the possible reason that the corresponding c-di-AMP·Cu^{2+} catalyzed D–A reactions give the similar activities and enantioselectivities in the presence of different additives.

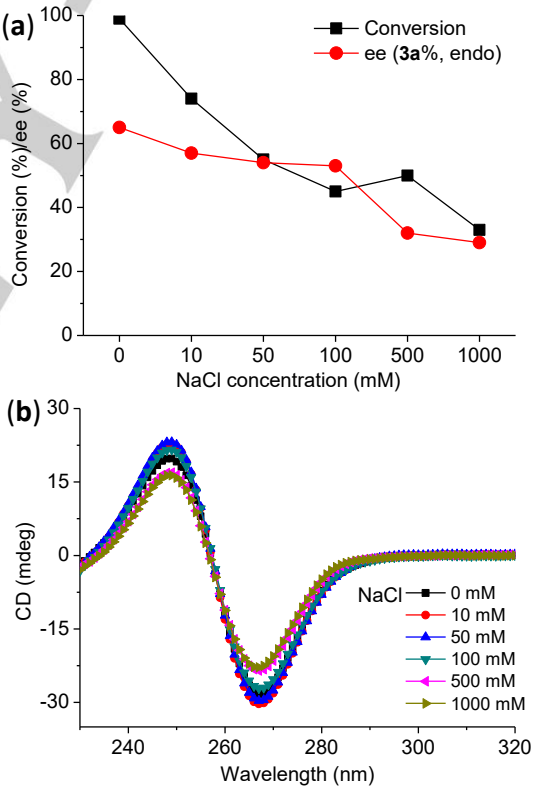

Figure 3. (a) c-di-AMP·Cu^{2+} catalyzed Diels–Alder reaction with Na^+ ions at varied concentrations (0-1000 mM) and (b) the corresponding CD spectra. Reaction condition: **1a** (2 μmol), **2** (250 μmol), c-di-AMP (250 μM), $Cu(OTf)_2$ (50 μM), MES buffer (500 μL, 20 mM, pH 5.5), 4 °C, 24 h.

We further examined the effect of Na^+ ions with different concentrations. Compared to c-di-AMP·Cu^{2+} without any additive, the conversions of **1a** are gradually decreasing when Na^+ ions are continuously added (Figure 3a). The *ee* values of **3a** (*endo*)

remain almost unchanged when the concentrations of Na^+ ions are below 100 mM, however, further increasing the amount of Na^+ ions causes an obvious decrement of the enantioselectivity (Figure 3a). In the corresponding CD spectra, the structures of c-di-AMP·Cu^{2+} change from compact state to a loose form when the amount of Na^+ ions is increasing (Figure 3b). The reduction of reactivity and enantioselectivity to c-di-AMP·Cu^{2+} catalyzed D–A reactions might be ascribed to the comparable unstable structure in high concentration of Na^+ ions, which shows the similar phenomena as described in G4DNA-based catalysis[4b, 4c, 5] and c-di-AMP based catalysis.[13] In short, the enantioselective catalytic properties of c-di-AMP·Cu^{2+} is less dependent on the additive species but largely dependent on their concentrations.

The effect of buffers

To optimize the buffer solution for the c-di-AMP·Cu^{2+} catalyzed D–A reaction, the effect of buffers was investigated with different species and pH values. For 4-morpholineethanesulfonic acid (MES) buffer at pH 4.5, the corresponding D–A reaction gives rise to 80% conversion and 53% *ee* (Table 2, entry 1). With increasing the pH value of MES buffer to 5.5, the conversion is increased to 98% and the *ee* value is up to 65% (Table 2, entry 2). However, further increment of the pH to 6.5 causes the reduced conversion and *ee* to the corresponding D–A reaction (Table 2, entry 3). The possible reason is ascribed to the protonation of c-di-AMP that may affect the interaction between c-di-AMP and Cu^{2+} ions. The similar phenomenon was also observed in the 4-morpholinepropanesulfonic acid (MOPS) buffer. With increasing the pH from 5.5 to 7.4 in MOPS buffer, the conversions of the corresponding reactions are gradually decreasing (Table 2, entries 4-7). The *ee* values of **3a** remain unchanged at pH 5.5 and 6.5, yet further increasing the pH provides the reduced enantioselectivities (Table 2, entries 4-7). In addition, phosphate buffer saline (PBS) and tris(hydroxymethyl)aminomethane (Tris) buffers at pH 7.4 generate the low conversions and *ee* values, which is comparable as that in MOPS buffer (Table 2, entry 7 vs. entries 8,9). These results indicate that high pH values cause negative effect to the c-di-AMP·Cu^{2+} catalyzed D–A reaction and MES buffer at pH 5.5 is screened as the optimal reaction medium.

Table 2. Enantioselective Diels–Alder reaction catalyzed by c-di-AMP·Cu^{2+} in different buffers.[a]

Entry	Buffer	pH	Conv. (%)	*endo*/*exo*	*ee* (**3a**%, *endo*)
1	MES	4.5	80	91:9	53
2		5.5	98	93:7	65
3		6.5	69	82:18	21
4	MOPS	5.5	89	94:6	57
5		6.5	81	94:6	58
6		7.0	50	91:9	29
7		7.4	18	92:8	22
8	PBS	7.4	9	83:17	19
9	Tris	7.4	8	75:25	5

[a] Reaction conditions: **1a** (2 μmol), **2** (250 μmol), c-di-AMP (250 μM), $Cu(OTf)_2$ (50 μM), buffer (500 μL, 20 mM), 4 °C, 24 h.

The effect of c-di-AMP analogues

Different c-di-AMP analogues were employed to examine the catalytic performance of CDN-based artificial metalloribozyme. With the assistance of Cu^{2+} ions as metal cofactors, the replacement of c-di-AMP to c-di-GMP causes a sharp decrease of the corresponding *ee* from 65% to 4% (Figure 4a). The distinct CD spectra of c-di-AMP and c-di-GMP might be the possible reason for the decreased enantioselectivity (Figure 4b). The other CDN of either c-di-CMP or c-di-UMP with different structures provides racemic **3a** in Cu^{2+}-involved D–A reaction (Figure 4). Compared to c-di-AMP, the c-AMP-GMP with only one substitution of one GMP still gives rise to a racemic D–A product (Figure 4a), which shows the different phenomenon as described in c-di-AMP based Friedel-Crafts reaction.[13] The possible reason might be attributed to the different reaction mechanisms between these two reactions. In addition, the non-structured 3',5'-cyclic AMP (cAMP), AMP and adenine in the presence of Cu^{2+} ions provide the racemic products (Figure 4). Briefly, the c-di-AMP analogue experiments indicate that Cu^{2+} ions can specifically bind to c-di-AMP to form an efficient metalloribozyme as described previously.[13]

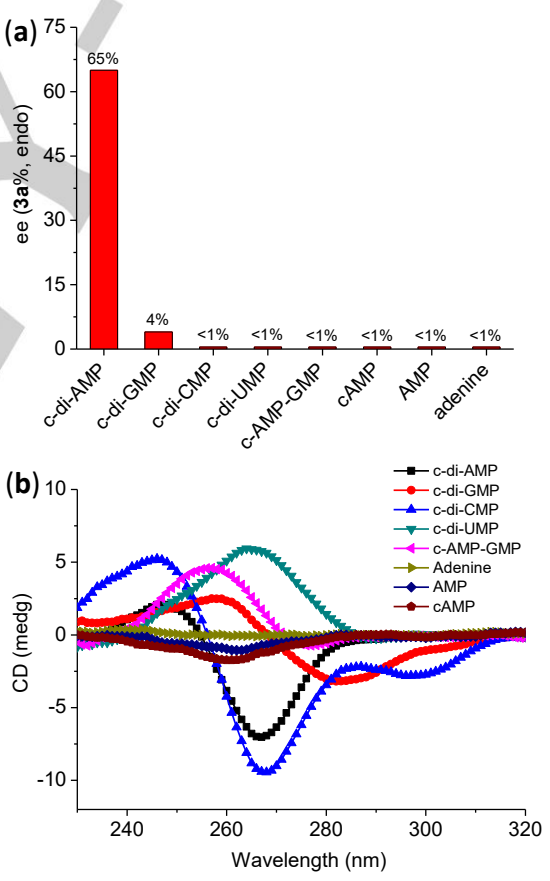

Figure 4. (a) The enantioselectivities of **3a** (*endo*) that were produced by Cu^{2+} in the presence of different c-di-AMP analogues. Reaction condition: **1a** (2 μmol), **2** (250 μmol), c-di-AMP analogue (250 μM), $Cu(OTf)_2$ (50 μM), MES buffer (500 μL, 20 mM, pH 5.5), 4 °C, 24 h. (b) CD spectra of different c-di-AMP analogues (250 μM) and $Cu(OTf)_2$ (50 μM) in MES buffer (20 mM, pH 5.5).

Kinetic study of the c-di-AMP·Cu^{2+}

In order to study the kinetic behavior of the c-di-AMP based metalloribozyme, we measured the apparent second-order rate constant (k_{app}) of the c-di-AMP·Cu^{2+} catalyzed benchmark D–A reaction. Compared to the uncatalyzed reaction, the Cu^{2+} ions provide a 65-fold rate acceleration (Table 3, entry 1 vs. entry 2). Once c-di-AMP and Cu^{2+} ions assemble into a c-di-AMP·Cu^{2+} metalloribozyme, the corresponding reaction rate improves about 300-fold compared to the uncatalyzed reaction and 5-fold compared to the bare Cu^{2+} ions (Table 3, entry 3). These results suggest that the presence of c-di-AMP not only contributes to the chiral induction but also provides a rate enhancement to the Cu^{2+}-involved D–A reaction. Furthermore, the rate acceleration effect of c-di-AMP·Cu^{2+} catalyzed D–A reaction is accordance with the phenomenon in c-di-AMP based Friedel-Crafts reaction,[13] resulting in an assumption of the possible synergistic effect between c-di-AMP and Cu^{2+} ions.

Table 3. The apparent second-order rate constants for the uncatalyzed and catalyzed Diels-Alder reactions.[a]

Entry	Catalyst	k_{app} (M^{-1} s^{-1})	k_{rel}
1	none	(1.2 ± 0.2) x 10^{-4}	1
2	Cu^{2+}	(7.8 ± 0.4) x 10^{-3}	65
3	c-di-AMP·Cu^{2+}	(3.8 ± 0.5) x 10^{-2}	317

[a] Reaction conditions: **1a** (50 μM), **2** (5 mM), c-di-AMP (250 μM), $Cu(OTf)_2$ (50 μM), MES buffer (2000 μL, 20 mM, pH 5.5), 4 °C. The rate acceleration effect $k_{rel} = k_{app,cat}/k_{app,uncat}$.

Substrate scope

In order to examine the substrate scope of the c-di-AMP·Cu^{2+} catalyzed D–A reactions, aza-chalcones with different substitutes were investigated. Compared to **1a** with R = Ph, either electro-donating or electro-withdrawing substitutions on the phenyl group provides reduced conversions and enantioselectivities (Table 4, entry 1 vs. entries 2-6), indicating that the substitutions in aza-chalcones cause negative effect to the enantioselective catalytic performance of c-di-AMP·Cu^{2+}. When the aza-chalcones bearing the electro-donating substitutions such as 4-Me and 4-OMe on the phenyl group (**1b** and **1c**), the corresponding D–A reactions provides the significant reduction of the conversions and the enantioselectivities (Table 4, entry 1 vs. entries 2-3). Once altering the methoxy substitution from 4'-position to 2'-position on the phenyl group (**1c** and **1d**), a further decreased conversion and enantioselectivity were obtained (Table 4, entry 3 vs. entry 4), indicating that c-di-AMP·Cu^{2+} exhibits an obvious steric effect to the aza-chalcone substrates. Compared to **1a**, the aza-chalcones with electro-withdrawing substituted phenyl group (**1e** and **1f**) results in a sharp decrement of the *ee* values to nearly racemic products, although the conversions remain almost unchanged (Table 4, entry 1 vs. entries 5-6). Intriguingly, aza-chalcones with the moieties of furyl (**1g**) and thienyl group (**1h**) show nearly quantitative conversions and good enantioselectivities up to 80% *ee* (Table 4, entries 7-8). The above results suggest that the c-di-AMP·Cu^{2+} is eligible for a series of aza-chalcone substrates in D–A reactions and the substitution in aza-chalcone substrates shows significant steric and electronic effect to the enantioselective catalytic performance of c-di-AMP·Cu^{2+}.

Table 4. Substrate scope of the c-di-AMP·Cu^{2+} catalyzed Diels–Alder reactions.[a]

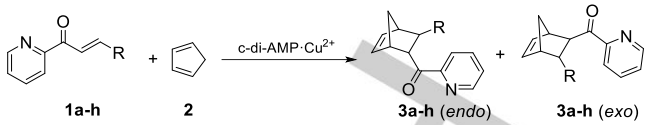

1a-h **2** **3a-h** (*endo*) **3a-h** (*exo*)

Entry	Aza-chalcone	R	Conv. (%)	*endo* /*exo*	*ee* (%, *endo*)
1[b]	**1a**		99	93:7	65
2	**1b**		85	97:3	45
3	**1c**		59	96:4	55
4	**1d**		42	95:5	23
5	**1e**		84	94:6	6
6	**1f**		90	90:10	5
7	**1g**		99	97:3	80
8	**1h**		97	96:4	80

[a] Reaction conditions: **1** (2 μmol), **2** (250 μmol), c-di-AMP (250 μM), $Cu(OTf)_2$ (50 μM), MES buffer (1 mL, 20 mM, pH 5.5), 4 °C, 3 d. [b] Reaction time 24 h.

Conclusion

In summary, we found that a c-di-AMP based artificial metalloribozyme could efficiently catalyze enantioselective D–A reactions with modest to good enantioselectivities. The enantioselective activity of c-di-AMP·Cu^{2+} is largely dependent on the metal cofactor, the molar ratio of c-di-AMP/Cu^{2+}, the additives and the buffers. In addition, a plausible synergistic effect between c-di-AMP and Cu^{2+} ions gives rise to a modest rate enhancement compared to Cu^{2+} ions. This work provides another example of CDN-based enantioselective catalysis and we anticipate that this work would promote the further exploration on RNA-based enantioselective catalysis and the possible catalytic roles of CDNs in early chemical evolution.

Experimental Section

General information

The cyclic dinucleotides of c-di-AMP, c-di-GMP, c-di-CMP, c-di-UMP and c-AMP-GMP were chemically synthesized using commercial phosphoramidites as starting materials according to the references.[16f, 19] 3',5'-Cyclic AMP, AMP and adenine were purchased from Sangon (Shanghai, China). The metal salts, achiral ligands and buffers were obtained from commercial sources and used without further purification. Water used was distilled and deionized using a Milli-Q A10 water

purification system. The aza-chalcones (**1a-h**) were synthesized followed by the reference.[20]

CD spectra were collected on a Chirascan circular dichroism spectrometer (Applied Photophysics Ltd, UK) from 230 to 320 nm using a 10 mm quartz cell with a scanning speed of 100 nm/min at 4 °C. UV-Vis spectra were measured on a HITACHI U-3900 spectrophotometer from 190 nm to 800 nm. The Diels-Alder reactions were analyzed by a chiral HPLC (Shimadzu Prominence-*i* LC-2030) using hexane and *iso*-propanol as eluents. Proton nuclear magnetic resonance (^{1}H NMR) and carbon nuclear magnetic resonance (^{13}C NMR) spectra were recorded on Bruker AV 600 and 400 MHz spectrometers using residue solvent peaks as an internal standard. High-resolution mass spectra (HRMS) were collected on a Bruker maxis system.

Synthesis of aza-chalcones and their racemic products

Synthesis of aza-chalcones (**1a**-**h**). For **1a**-**d**: 2-acetylpyridine (8.25 mmol) and the appropriate benzaldehyde (8.25 mmol) were introduced in 50 mL of distilled water at 4 °C after stirring for 0.5 h. Then, 5 mL of sodium hydroxide solution (10 wt%) was added. After stirring for another 0.5 h and left the mixture to stand overnight at 4 °C. The reaction mixture was filtered and washed by water to provide the crude products with >90% yields. The pure products were obtained by recrystallization in ethanol. For **1e**-**h**: To a stirred solution of 0.5 mL of 10% aqueous sodium hydroxide and the appropriate aldehyde (8.25 mmol) in 10 mL of ethanol, 2-acetylpyridine (8.25 mmol) was added dropwise after stirring for 1 h. After being stirred for another 2 h at 0 °C, the reaction mixture was filtered and nearly pure product was obtained with >90% yields.

(*E*)-3-phenyl-1-(pyridin-2-yl)prop-2-en-1-one (1a): ^{1}H NMR (600 MHz, $CDCl_3$) δ 8.75 (s, 1H), 8.31 (d, *J* = 16.0 Hz, 1H), 8.19 (d, *J* = 7.7 Hz, 1H), 7.94 (d, *J* = 16.0 Hz, 1H), 7.87 (td, *J* = 7.7, 1.5 Hz, 1H), 7.73 (dd, *J* = 6.8, 2.3 Hz, 2H), 7.58 – 7.34 (m, 4H). ^{13}C NMR (150 MHz, $CDCl_3$) δ 189.48 (s), 154.23 (s), 148.84 (s), 144.81 (s), 137.04 (s), 135.18 (s), 130.57 (s), 128.86 (d, *J* = 3.4 Hz), 126.91 (s), 122.95 (s), 120.92 (s). HRMS (ESI) calcd. For $[C_{14}H_{11}NO]\cdot Na^+$ $(M+Na)^+$: *m/z* 232.0733, found 232.0731.

(*E*)-1-(pyridin-2-yl)-3-p-tolylprop-2-en-1-one (1b): ^{1}H NMR (400 MHz, $CDCl_3$) δ 8.75 – 8.66 (m, 1H), 8.24 (d, *J* = 16.0 Hz, 1H), 8.16 (d, *J* = 7.9 Hz, 1H), 7.91 (d, *J* = 16.0 Hz, 1H), 7.82 (td, *J* = 7.7, 1.7 Hz, 1H), 7.60 (d, *J* = 8.1 Hz, 2H), 7.43 (ddd, *J* = 7.5, 4.8, 1.1 Hz, 1H), 7.18 (d, *J* = 8.0 Hz, 2H), 2.35 (s, 3H). ^{13}C NMR (100 MHz, $CDCl_3$) δ 189.44 (s), 154.34 (s), 148.82 (s), 144.85 (s), 141.09 (s), 136.96 (s), 132.45 (s), 129.63 (s), 128.88 (s), 126.79 (s), 122.86 (s), 119.86 (s), 21.55 (s). HRMS (ESI) calcd. For $[C_{15}H_{13}NO]\cdot Na^+$ $(M+Na)^+$: *m/z* 246.0889, found 246.0884.

(*E*)-3-(4-methoxyphenyl)-1-(pyridin-2-yl)prop-2-en-1-one (1c): ^{1}H NMR (400 MHz, $CDCl_3$) δ 8.78 – 8.70 (m, 1H), 8.19 (dd, *J* = 11.9, 4.0 Hz, 2H), 7.89 (ddd, *J* = 13.2, 9.4, 8.8 Hz, 2H), 7.70 (d, *J* = 8.7 Hz, 2H), 7.48 (ddd, *J* = 7.5, 4.8, 1.1 Hz, 1H), 6.94 (d, *J* = 8.7 Hz, 2H), 3.86 (s, 3H). ^{13}C NMR (100 MHz, $CDCl_3$) δ 189.31 (s), 161.77 (s), 148.72 (s), 144.78 (s), 137.07 (s), 130.68 (s), 128.00 (s), 126.73 (s), 122.92 (s), 118.55 (s), 114.35 (s), 55.41 (s). HRMS (ESI) calcd. For $[C_{15}H_{13}NO_2]\cdot Na^+$ $(M+Na)^+$: *m/z* 262.0838, found 262.0831.

(*E*)-3-(2-methoxyphenyl)-1-(pyridin-2-yl)prop-2-en-1-one (1d): ^{1}H NMR (600 MHz, $CDCl_3$) δ 8.74 (s, 1H), 8.32 (q, *J* = 16.2 Hz, 2H), 8.18 (d, *J* = 7.8 Hz, 1H), 7.86 (td, *J* = 7.7, 1.6 Hz, 1H), 7.79 (dd, *J* = 7.7, 1.4 Hz, 1H), 7.47 (dd, *J* = 6.8, 5.0 Hz, 1H), 7.44 – 7.33 (m, 1H), 6.99 (t, *J* = 7.5 Hz, 1H), 6.93 (d, *J* = 8.3 Hz, 1H), 3.91 (s, 3H). ^{13}C NMR (150 MHz, $CDCl_3$) δ 189.79 (s), 158.91 (s), 154.55 (s), 148.82 (s), 139.99 (s), 136.97 (s), 131.92 (s), 128.84 (s), 126.71 (s), 124.22 (s), 122.93 (s), 121.11 (s), 120.67 (s), 111.19 (s), 55.59 (s). HRMS (ESI) calcd. For $[C_{15}H_{13}NO_2]\cdot Na^+$ $(M+Na)^+$: *m/z* 262.0838, found 262.0833.

(*E*)-3-(4-chlorophenyl)-1-(pyridin-2-yl)prop-2-en-1-one (1e): ^{1}H NMR (400 MHz, $CDCl_3$) δ 8.73 (d, *J* = 4.6 Hz, 1H), 8.27 (d, *J* = 16.1 Hz, 1H), 8.18 (d, *J* = 7.9 Hz, 1H), 7.87 (dd, *J* = 8.7, 7.3 Hz, 2H), 7.65 (d, *J* = 8.4 Hz, 2H), 7.54 – 7.46 (m, 1H), 7.38 (d, *J* = 8.4 Hz, 2H). ^{13}C NMR (100 MHz, $CDCl_3$) δ 189.29 (s), 154.06 (s), 148.88 (s), 143.19 (s), 137.07 (s), 136.43 (s), 133.68 (s), 129.96 (s), 129.16 (s), 127.01 (s), 122.96 (s), 121.36 (s). HRMS (ESI) calcd. For $[C_{14}H_{10}NOCl]\cdot Na^+$ $(M+Na)^+$: *m/z* 266.0343, found 266.0336.

(*E*)-3-(4-nitrophenyl)-1-(pyridin-2-yl)prop-2-en-1-one (1f): ^{1}H NMR (400 MHz, $CDCl_3$) δ 8.72 (dd, *J* = 3.5, 1.1 Hz, 1H), 8.39 (d, *J* = 16.1 Hz, 1H), 8.28 – 8.20 (m, 2H), 8.16 (dd, *J* = 7.8, 0.7 Hz, 1H), 7.85 (ddd, *J* = 17.6, 8.2, 6.7 Hz, 4H), 7.50 (ddd, *J* = 7.5, 4.7, 1.1 Hz, 1H). ^{13}C NMR (100 MHz, $CDCl_3$) δ 188.88 (s), 153.57 (s), 148.97 (s), 148.52 (s), 141.25 (d, *J* = 11.1 Hz), 137.19 (s), 129.23 (s), 127.33 (s), 124.82 (s), 124.10 (s), 123.05 (s). HRMS (ESI) calcd. For $[C_{14}H_{10}N_2O_3]\cdot Na^+$ $(M+Na)^+$: *m/z* 277.0584, found 277.0573.

(*E*)-3-(furan-2-yl)-1-(pyridin-2-yl)prop-2-en-1-one (1g): ^{1}H NMR (600 MHz, $CDCl_3$) δ 8.82 – 8.67 (m, 1H), 8.14 (dd, *J* = 18.8, 11.8 Hz, 2H), 7.85 (td, *J* = 7.7, 1.7 Hz, 1H), 7.69 (d, *J* = 15.8 Hz, 1H), 7.53 (d, *J* = 1.1 Hz, 1H), 7.46 (ddd, *J* = 7.5, 4.7, 1.0 Hz, 1H), 6.76 (d, *J* = 3.4 Hz, 1H), 6.50 (dd, *J* = 3.3, 1.7 Hz, 1H). ^{13}C NMR (150 MHz, $CDCl_3$) δ 189.32 (s), 154.22 (s), 152.12 (s), 148.92 (s), 145.12 (s), 136.96 (s), 130.68 (s), 126.81 (s), 122.81 (s), 118.75 (s), 116.21 (s), 112.65 (s). HRMS (ESI) calcd. For $[C_{14}H_{10}N_2O_3]\cdot Na^+$ $(M+Na)^+$: *m/z* 222.0525, found 222.0524.

(*E*)-1-(pyridin-2-yl)-3-(thiophen-2-yl)prop-2-en-1-one (1h): ^{1}H NMR (600 MHz, $CDCl_3$) δ 8.73 (d, *J* = 4.6 Hz, 1H), 8.16 (d, *J* = 7.8 Hz, 1H), 8.05 (s, 2H), 7.85 (td, *J* = 7.7, 1.5 Hz, 1H), 7.49 – 7.44 (m, 1H), 7.41 (dd, *J* = 13.3, 4.3 Hz, 2H), 7.08 (dd, *J* = 4.7, 3.9 Hz, 1H). ^{13}C NMR (150 MHz, $CDCl_3$) δ 189.12 (s), 154.16 (s), 148.87 (s), 140.90 (s), 137.14 (s), 137.00 (s), 132.16 (s), 129.21 (s), 128.29 (s), 126.86 (s), 122.85 (s), 119.87 (s). HRMS (ESI) calcd. For $[C_{12}H_9NOS]\cdot Na^+$ $(M+Na)^+$: *m/z* 238.0297, found 238.0293.

Synthesis of the racemates (**3a**-**h**). To a stirred solution of $Cu(OTf)_2$ (0.11 mmol) in H_2O (5 mL), aza-chalcone **1** (0.19 mmol) in CH_3CN and cyclopentadiene (1 mL) were added. The reaction mixture was stirred at room temperature until the completion of the reaction as monitored by TLC. The reaction mixture was extracted with ethyl acetate (3 x 15 mL) and the combined organic layer was dried over anhydrous Na_2SO_4. The solvent was removed under reduced pressure and the crude residue was purified by flash chromatography on silica gel (0–30% EtOAc/petrol ether) to afford the pure product.

(3-Phenylbicyclo[2.2.1]hept-5-en-2-yl)(pyridin-2-yl)methanone (3a): ^{1}H NMR (400 MHz, $CDCl_3$) δ 8.78 – 8.59 (m, 1H), 8.11 – 7.97 (m, 1H), 7.79 (td, *J* = 7.7, 1.7 Hz, 1H), 7.42 (ddd, *J* = 7.6, 4.8, 1.3 Hz, 1H), 7.30 (ddd, *J* = 13.2, 8.3, 1.3 Hz, 4H), 7.17 (ddd, *J* = 8.5, 2.6, 1.3 Hz, 1H), 6.51 (dd, *J* = 5.6, 3.2 Hz, 1H), 5.85 (dd, *J* = 5.6, 2.8 Hz, 1H), 4.56 (dd, *J* = 5.2, 3.4 Hz, 1H), 3.64 – 3.43 (m, 2H), 3.10 (d, *J* = 1.4 Hz, 1H), 2.09 (d, *J* = 8.6 Hz, 1H), 1.68 – 1.55 (m, 1H). ^{13}C NMR (100 MHz, $CDCl_3$) δ 201.17 (s), 153.68 (s), 148.99 (s), 144.75 (s), 139.53 (s), 136.95 (s), 132.99 (s), 128.51 (s), 127.77 (s), 127.02 (s), 125.96 (s), 122.29 (s), 54.40 (s), 49.47 (s), 48.89 (s), 48.36 (s), 45.69 (s). HRMS (ESI) calcd. For $[C_{19}H_{17}NO]\cdot Na^+$ $(M+Na)^+$: *m/z* 298.1202, found 298.1199.

Pyridin-2-yl(3-p-tolylbicyclo[2.2.1]hept-5-en-2-yl)methanone (3b): ^{1}H NMR (400 MHz, $CDCl_3$) δ 8.68 (ddd, J = 4.7, 1.6, 0.8 Hz, 1H), 8.03 – 7.96 (m, 1H), 7.81 (td, J = 7.7, 1.7 Hz, 1H), 7.45 (ddd, J = 7.5, 4.8, 1.2 Hz, 1H), 7.22 (d, J = 8.1 Hz, 2H), 7.09 (d, J = 8.0 Hz, 2H), 6.49 (dd, J = 5.5, 3.1 Hz, 1H), 5.82 (dd, J = 5.6, 2.8 Hz, 1H), 4.52 (dd, J = 5.2, 3.4 Hz, 1H), 3.54 (s, 1H), 3.41 (d, J = 4.5 Hz, 1H), 3.05 (d, J = 1.4 Hz, 1H), 2.29 (d, J = 9.0 Hz, 3H), 2.07 (d, J = 8.4 Hz, 1H), 1.63 – 1.54 (m, 1H). ^{13}C NMR (100 MHz, $CDCl_3$) δ 201.18 (s), 153.66 (s), 148.85 (s), 141.55 (s), 139.46 (s), 136.82 (s), 135.30 (s), 132.77 (s), 129.05 (s), 127.56 (s), 126.84 (s), 122.18 (s), 54.18 (s), 49.61 (s), 48.72 (s), 48.21 (s), 45.31 (s), 20.90 (s). HRMS (ESI) calcd. For $[C_{20}H_{19}NO]\cdot Na^+$ $(M+Na)^+$: *m/z* 312.1359, found 312.1354.

(3-(4-Methoxyphenyl)bicyclo[2.2.1]hept-5-en-2-yl)(pyridin-2-yl)methanone (3c): ^{1}H NMR (400 MHz, $CDCl_3$) δ 8.68 (dd, *J* = 4.7, 0.7 Hz, 1H), 8.00 (d, *J* = 7.8 Hz, 1H), 7.81 (td, *J* = 7.7, 1.7 Hz, 1H), 7.45 (ddd, *J* = 7.5, 4.8, 1.2 Hz, 1H), 7.24 (d, *J* = 8.6 Hz, 2H), 6.88 – 6.77 (m, 2H), 6.48 (dd, *J* = 5.5, 3.2 Hz, 1H), 5.82 (dd, *J* = 5.6, 2.7 Hz, 1H), 4.49 (dd, *J* = 5.1, 3.4 Hz, 1H), 3.76 (d, *J* = 7.6 Hz, 3H), 3.53 (s, 1H), 3.38 (d, *J* = 5.0 Hz, 1H), 3.02 (s, 1H), 2.06 (d, *J* = 8.4 Hz, 1H), 1.74 – 1.51 (m, 2H), 1.26 (s, 1H). ^{13}C NMR (100 MHz, $CDCl_3$) δ 201.21 (s), 157.77 (s), 153.65 (s), 148.85 (s), 139.45 (s), 136.76 (d, *J* = 15.3 Hz), 132.74 (s), 128.55 (s), 126.85 (s), 122.18 (s), 113.79 (s), 55.28 (s), 54.30 (s), 49.68 (s), 48.69 (s), 48.17 (s), 44.93 (s). HRMS (ESI) calcd. For $[C_{20}H_{19}NO_2]\cdot Na^+$ $(M+Na)^+$: *m/z* 328.1308, found 328.1303.

(3-(2-Methoxyphenyl)bicyclo[2.2.1]hept-5-en-2-yl)(pyridin-2-yl)methanone (3d): ^{1}H NMR (400 MHz, $CDCl_3$) δ 8.63 (d, *J* = 4.5 Hz), 8.09 (d, *J* = 7.8 Hz), 7.82 (tt, *J* = 8.3, 4.1 Hz), 7.48 – 7.38 (m), 7.34 (dd, *J* = 10.2, 6.4 Hz), 7.20 – 7.11 (m), 6.93 (t, *J* = 7.3 Hz), 6.71 (t, *J* = 8.9 Hz), 6.48 (dd, *J* = 5.5, 3.3 Hz), 5.92 (dd, *J* = 5.6, 2.8 Hz), 4.37 (dd, *J* = 5.1, 3.4 Hz), 3.42 (s), 3.32 (d, *J* = 10.5 Hz), 3.31 – 3.24 (m), 1.95 (d, *J* = 8.3 Hz), 1.61 (dd, *J* = 8.3, 1.7 Hz). ^{13}C NMR (100 MHz, $CDCl_3$) δ 200.83 (s), 157.73 (s), 154.06 (s), 148.92 (s), 138.03 (s), 136.86 (s), 133.86 (s), 133.60 (s), 126.72 (d, *J* = 12.9 Hz), 125.87 (s), 122.00 (s), 120.28 (s), 109.84 (s), 54.66 (s), 52.11 (s), 48.36 (d, *J* = 15.5 Hz), 46.39 (s), 41.74 (s), 29.81 (s). HRMS (ESI) calcd. For $[C_{20}H_{19}NO_2]\cdot Na^+$ $(M+Na)^+$: *m/z* 328.1308, found 328.1301.

(3-(4-Chlorophenyl)bicyclo[2.2.1]hept-5-en-2-yl)(pyridin-2-yl)methanone (3e): ^{1}H NMR (400 MHz, $CDCl_3$) δ 8.60 (d, *J* = 4.6 Hz, 1H), 7.93 (d, *J* = 7.8 Hz, 1H), 7.76 (t, *J* = 7.7 Hz, 1H), 7.43 – 7.32 (m, 1H), 7.18 (d, *J* = 10.5 Hz, 5H), 6.41 (d, *J* = 3.8 Hz, 1H), 5.82 – 5.69 (m, 1H), 4.45 – 4.33 (m, 1H), 3.47 (s, 1H), 3.33 (d, *J* = 4.9 Hz, 1H), 2.98 (s, 1H), 1.94 (d, *J* = 8.5 Hz, 1H), 1.70 – 1.62 (m, 1H). ^{13}C NMR (100 MHz, $CDCl_3$) δ 148.87 (s), 139.25 (s), 136.91 (s), 133.00 (s), 128.96 (s), 128.42 (s), 127.68 – 127.15 (m), 122.23 (s), 54.45 (s), 49.27 (s), 48.71 (s), 48.16 (s), 45.10 (s), 29.70 (s), 13.72 (s). HRMS (ESI) calcd. For $[C_{19}H_{16}NOCl]\cdot Na^+$ $(M+Na)^+$: *m/z* 332.0813, found 332.0806.

(3-(4-Nitrophenyl)bicyclo[2.2.1]hept-5-en-2-yl)(pyridin-2-yl)methanone (3f): ^{1}H NMR (400 MHz, $CDCl_3$) δ 8.69 – 8.63 (m, 1H), 8.13 (d, *J* = 8.6 Hz, 2H), 8.01 (d, *J* = 7.8 Hz, 1H), 7.83 (dd, *J* = 10.9, 4.5 Hz, 1H), 7.51 – 7.40 (m, 3H), 6.48 (dd, *J* = 5.4, 3.3 Hz, 1H), 5.87 (dd, *J* = 5.5, 2.7 Hz, 1H), 4.53 – 4.41 (m, 1H), 3.60 (s, 1H), 3.53 (d, *J* = 5.1 Hz, 1H), 3.12 (s, 1H), 2.00 (d, *J* = 8.6 Hz, 1H), 1.67 (d, *J* = 8.4 Hz, 2H). ^{13}C NMR (100 MHz, $CDCl_3$) δ 200.39 (s), 153.24 (s), 152.81 (s), 148.92 (s), 138.97 (s), 137.01 (s), 133.43 (s), 128.37 (s), 127.18 (s), 123.64 (s), 122.32 (s), 54.71 (s), 48.86 (d, *J* = 19.0 Hz), 48.20 (s), 45.76 (s). HRMS (ESI) calcd. For $[C_{19}H_{16}N_2O_3]\cdot Na^+$ $(M+Na)^+$: *m/z* 343.1053, found 343.1044.

(3-(Furan-2-yl)bicyclo[2.2.1]hept-5-en-2-yl)(pyridin-2-yl)methanone (3g): ^{1}H NMR (400 MHz, $CDCl_3$) δ 8.78 – 8.63 (m), 8.05 – 7.94 (m), 7.88 – 7.76 (m), 7.47 (ddd, *J* = 7.5, 4.8, 1.2 Hz), 7.36 – 7.27 (m), 6.43 (ddd, *J* = 18.2, 5.5, 3.2 Hz), 6.27 (dd, *J* = 3.1, 1.9 Hz), 6.10 (t, *J* = 4.4 Hz), 5.79 (dd, *J* = 5.6, 2.8 Hz), 4.59 (dd, *J* = 4.9, 3.6 Hz), 3.53 (s), 3.39 (d, *J* = 4.3 Hz), 3.07 (d, *J* = 1.3 Hz), 2.04 (d, *J* = 8.3 Hz), 1.61 – 1.48 (m). ^{13}C NMR (100 MHz, $CDCl_3$) δ 200.45 (s), 158.18 (s), 153.46 (s), 148.99 (s), 141.16 (s), 138.46 (s), 136.98 (s), 132.90 (s), 127.08 (s), 122.35 (s), 110.13 (s), 104.89 (s), 52.22 (s), 49.22 (s), 48.66 (s), 48.33 (s), 39.75 (s), 29.81 (s). HRMS (ESI) calcd. For $[C_{19}H_{16}N_2O_3]\cdot Na^+$ $(M+Na)^+$: *m/z* 288.0995, found 288.0984.

Pyridin-2-yl(3-(thiophen-2-yl)bicyclo[2.2.1]hept-5-en-2-yl)methanone (3h): ^{1}H NMR (400 MHz, $CDCl_3$) δ 8.70 (d, *J* = 4.3 Hz), 8.00 (d, *J* = 7.9 Hz), 7.82 (td, *J* = 7.7, 1.7 Hz), 7.46 (ddd, *J* = 7.6, 4.9, 1.2 Hz), 7.15 – 7.08 (m), 6.96 – 6.86 (m), 6.45 (dd, *J* = 5.5, 3.2 Hz), 5.80 (dd, *J* = 5.6, 2.8 Hz), 4.58 (dd, *J* = 4.9, 3.5 Hz), 3.70 – 3.51 (m), 3.06 (s), 2.12 (d, *J* = 8.7 Hz), 1.64 (dd, *J* = 8.7, 1.7 Hz). ^{13}C NMR (100 MHz, $CDCl_3$) δ 200.50 (s), 153.46 (s), 149.06 (d, *J* = 9.5 Hz), 138.77 (s), 136.94 (s), 132.77 (s), 127.08 (s), 126.75 (s), 123.78 (s), 123.07 (s), 122.31 (s), 55.77 (s), 51.60 (s), 48.66 (d, *J* = 3.6 Hz), 41.67 (s). HRMS (ESI) calcd. For $[C_{17}H_{15}NOS]\cdot Na^+$ $(M+Na)^+$: *m/z* 304.0767, found 304.0761.

Typical procedure

To a 10 mL vial, a stock solution of c-di-AMP (final conc. 250 μM) and a freshly prepared solution of $Cu(OTf)_2$ (final conc. 50 μM) were successively added to a MES buffer (20 mM, pH 5.5) to make a total volume of 500 μL. After stirred for 30 min at 4 °C, a thoroughly mixed solution of aza-chalcone **1** (10 μL of 0.1 M stock solution in CH_3CN or DMSO, 2 μmol) and freshly distilled cyclopentadiene **2** (21 μL, 250 μmol) were added immediately. After the mixture was stirred for 3 days (**1a** for 24 h) at 4 °C, the aqueous media was extracted by diethyl ether (3 × 2 mL) and flushed on a short gel column. The combined organic solvent was removed under reduced pressure and the residue was directly analyzed by chiral HPLC with the eluents of hexane and isopropanol using Daicel chiralpak columns (OD, ODH, AD, 250 × 4.6 mm). All data are averaged over two individual experiments. The *endo/exo* and the *ee* were determined by the chiral HPLC with the reproducibility of ±5%. The conversions of **1b-h** were roughly estimated form the crude ^{1}H-NMR with the reproducibility of ±10%. The conversion of **1a** was calculated from the HPLC with the reproducibility of ±5% by the following equation as described previously.[4b]

$$\text{Conversion of } \mathbf{1a}\ (\%) = A_{\mathbf{3a}}/(A_{\mathbf{3a}} + A_{\mathbf{1a}}/f)$$

where $A_{\mathbf{1a}}$ and $A_{\mathbf{3a}}$ are the HPLC areas of **1a** and **3a**, respectively. *f* is the correction factor of 0.595 from a fitting curve (Figure S5).

Kinetic study

The kinetic studies of c-di-AMP·Cu^{2+} catalyzed Diels-Alder reactions were evaluated upon the initial rate V_{init} and the apparent second-order rate constant k_{app} as described in the literature.[20] The V_{init} of the Diels-Alder reaction between **1a** and **2** was determined on a UV-Vis spectrometer (Agilent Cary 3500) by monitoring the disappearance of the absorption of **1a** at 326 nm. To a 3 mL quartz cuvette (1 cm path length), a small magnet was placed followed by the addition of an aqueous solution of MES buffer (2 mL, 20 mM, pH 5.5) containing c-di-AMP (250 μM) and $Cu(OTf)_2$ (50 μM). After stirring for 30 min at 4 °C, a mixture of **1a** (10 μL of 10 mM **1a** in CH_3CN, 0.1 μmol) and freshly distilled cyclopentadiene **2** (10 μL of 1.0 M **2** in CH_3CN, 10 μmol) was added and the UV absorbance at 326 nm was started to collect every 20 seconds with continuous stirring at 4 °C. The V_{init} was calculated by the following equation:

$$V_{init} = d[A_{\mathbf{1a}}]/dt\cdot(d\cdot(\varepsilon_{\mathbf{1a}} - \varepsilon_{\mathbf{3a}}))^{-1}$$

where $d[A_{\mathbf{1a}}]/dt$ is the slope of the UV absorbance of **1a** at 326 nm *vs.* time during the initial conversion below 15%, d is the path length of the cuvette, $\varepsilon_{\mathbf{1a}}$ and $\varepsilon_{\mathbf{3a}}$ are the molar extinction coefficients of **1a** and **3a**, respectively.

The apparent second-order rate constant k_{app} was determined based on the V_{init} using the following equation:

$$k_{app} = V_{init}/([\mathbf{1a}]_0\cdot[\mathbf{2}]_0)$$

where $[\mathbf{1a}]_0$ and $[\mathbf{2}]_0$ are the initial concentrations of **1a** and **2**, respectively.

The rate acceleration effect k_{rel} was estimated by the ratio of $k_{app,cat}/k_{app,uncat}$,

$$k_{rel} = k_{app,cat}/k_{app,uncat}$$

where $k_{app,cat}$ and $k_{app,uncat}$ are the apparent second-order rate constants with and without catalyst, respectively.

Acknowledgements

This work was financially supported by the National Natural Science Foundation of China (21703132, 21773149, 21273142), the Natural Science Foundation of Shaanxi Province of China (2019JQ161) and the Fundamental Research Funds for the Central Universities (GK201802001).

Keywords: metalloribozyme • c-di-AMP • enantioselective catalysis • Diels-Alder reaction • primordial chemistry

[1] G. Roelfes, B. L. Feringa, *Angew. Chem. Int. Ed.* **2005**, *44*, 3230-3232; *Angew. Chem.* **2005**, *117*, 3294-3296.

[2] a) D. Coquiere, B. L. Feringa, G. Roelfes, *Angew. Chem. Int. Ed.* **2007**, *46*, 9308-9311; *Angew. Chem.* **2007**, *119*, 9468-9671; b) N. Shibata, H. Yasui, S. Nakamura, T. Toru, *Synlett* **2007**, 1153-1157; c) E. W. Dijk, B. L. Feringa, G. Roelfes, *Tetrahedron-Asymmetry* **2008**, *19*, 2374-2377; d) A. J. Boersma, B. L. Feringa, G. Roelfes, *Angew. Chem. Int. Ed.* **2009**, *48*, 3346-3348; *Angew. Chem.* **2009**, *121*, 4490-4493; e) A. J. Boersma, D. Coquiere, D.

Geerdink, F. Rosati, B. L. Feringa, G. Roelfes, *Nat. Chem.* **2010**, *2*, 991-995; f) R. P. Megens, G. Roelfes, *Chem. Commun.* **2012**, *48*, 6366-6368; g) Y. Li, C. Wang, G. Jia, S. Lu, C. Li, *Tetrahedron* **2013**, *69*, 6585-6590; h) A. Garcia-Fernandez, R. P. Megens, L. Villarino, G. Roelfes, *J. Am. Chem. Soc.* **2016**, *138*, 16308-16314.

[3] a) P. Fournier, R. Fiammengo, A. Jaeschke, *Angew. Chem. Int. Ed.* **2009**, *48*, 4426-4429; A*ngew. Chem.* **2009**, *121*, 4490-4493; b) J. Oelerich, G. Roelfes, *Chem. Sci.* **2013**, *4*, 2013-2017; c) A. Rioz-Martinez, J. Oelerich, N. Segaud, G. Roelfes, *Angew. Chem. Int. Ed.* **2016**, *55*, 14136-14140; *Angew. Chem.* **2016**, *128*, 14342-14346.

[4] a) S. Roe, D. J. Ritson, T. Garner, M. Searle, J. E. Moses, *Chem. Commun.* **2010**, *46*, 4309-4311; b) C. Wang, G. Jia, J. Zhou, Y. Li, Y. Liu, S. Lu, C. Li, *Angew. Chem. Int. Ed.* **2012**, *51*, 9352-9355; *Angew. Chem.* **2012**, *124*, 9486-9489; c) C. Wang, Y. Li, G. Jia, Y. Liu, S. Lu, C. Li, *Chem. Commun.* **2012**, *48*, 6232-6234; d) M. Wilking, U. Hennecke, *Org. Biomol. Chem.* **2013**, *11*, 6940-6945; e) Y. Li, G. Jia, C. Wang, M. Cheng, C. Li, *ChemBioChem* **2015**, *16*, 618-624; f) S. Dey, A. Jaeschke, *Angew. Chem. Int. Ed.* **2015**, *54*, 11279-11282; *Angew. Chem.* **2015**, *127*, 11432-11436; g) Y. Li, M. Cheng, J. Hao, C. Wang, G. Jia, C. Li, *Chem. Sci.* **2015**, *6*, 5578-5585; h) M. Cheng, Y. Li, J. Zhou, G. Jia, S.-M. Lu, Y. Yang, C. Li, *Chem. Commun.* **2016**, *52*, 9644-9647; i) S. Dey, C. L. Ruehl, A. Jaeschke, *Chem. Eur. J.* **2017**, *23*, 12162-12170.

[5] C. Wang, G. Jia, Y. Li, S. Zhang, C. Li, *Chem. Commun.* **2013**, *49*, 11161-11163.

[6] X. Xu, W. Mao, F. Lin, J. Hu, Z. He, X. Weng, C.-J. Wang, X. Zhou, *Catal. Commun.* **2016**, *74*, 16-18.

[7] M. Chandra, S. K. Silverman, *J. Am. Chem. Soc.* **2008**, *130*, 2936-2937.

[8] a) S. Park, L. Zheng, S. Kumakiri, S. Sakashita, H. Otomo, K. Ikehata, H. Sugiyama, *ACS Catal.* **2014**, *4*, 4070-4073; b) M. Su, M. Tomas-Gamasa, T. Carell, *Chem. Sci.* **2015**, *6*, 632-638; c) J. J. Marek, R. P. Singh, A. Heuer, U. Hennecke, *Chem. Eur. J.* **2017**, *23*, 6004-6008.

[9] J. Bai, X. Sun, H. Wang, C. Li, R. Qiao, *J. Org. Chem.* **2020**, *85*, 2010-2018.

[10] B. Seelig, S. Keiper, F. Stuhlmann, A. Jaschke, *Angew. Chem. Int. Ed.* **2000**, *39*, 4576-4579; *Angew. Chem.* **2000**, *112*, 4764-4768.

[11] N. Duchemin, E. Benedetti, L. Bethge, S. Vonhoff, S. Klussmann, J.-J. Vasseur, J. Cossy, M. Smietana, S. Arseniyadis, *Chem. Commun.* **2016**, *52*, 8604-8607.

[12] J. J. Marek, U. Hennecke, *Chem. Eur. J.* **2017**, *23*, 6009-6013.

[13] C. Wang, M. Hao, Q. Qi, J. Dang, X. Dong, S. Lv, L. Xiong, H. Gao, G. Jia, Y. Chen, J. S. Hartig, C. Li, *Angew. Chem. Int. Ed.* **2020**, *59*, 3444-3447; *Angew. Chem.* **2020**, *132*, 3472-3477.

[14] a) R. Hengge, *Nat. Rev. Microbiol.* **2009**, *7*, 263-273; b) R. M. Corrigan, A. Gruendling, *Nat. Rev. Microbiol.* **2013**, *11*, 513-524; c) U. Romling, M. Y. Galperin, M. Gomelsky, *Microbiol. Mol. Biol. Rev.* **2013**, *77*, 1-52.

[15] a) P. Ross, H. Weinhouse, Y. Aloni, D. Michaeli, P. Weinbergerohana, R. Mayer, S. Braun, E. Devroom, G. A. Vandermarel, J. H. Vanboom, M. Benziman, *Nature* **1987**, *325*, 279-281; b) G. Witte, S. Hartung, K. Buttner, K. P. Hopfner, *Mol. Cell* **2008**, *30*, 167-178; c) B. W. Davies, R. W. Bogard, T. S. Young, J. J. Mekalanos, *Cell* **2012**, *149*, 358-370; d) P. Gao, M. Ascano, Y. Wu, W. Barchet, B. L. Gaffney, T. Zillinger, A. A. Serganov, Y. Liu, R. A. Jones, G. Hartmann, T. Tuschl, D. J. Patel, *Cell* **2013**, *153*, 1094-1107; e) A. T. Whiteley, J. B. Eaglesham, C. C. d. O. Mann, B. R. Morehouse, B. Lowey, E. A. Nieminen, O. Danilchanka, D. S. King, A. S. Y. Lee, J. J. Mekalanos, P. J. Kranzusch, *Nature* **2019**, *567*, 194-199.

[16] a) Z. Y. Zhang, S. Kim, B. L. Gaffney, R. A. Jones, *J. Am. Chem. Soc.* **2006**, *128*, 7015-7024; b) S. Nakayama, I. Kelsey, J. Wang, K. Roelofs, B. Stefane, Y. Luo, V. T. Lee, H. O. Sintim, *J. Am. Chem. Soc.* **2011**, *133*, 4856-4864; c) S. Nakayama, I. Kelsey, J. Wang, H. O. Sintim, *Chem. Commun.* **2011**, *47*, 4766-4768; d) S. Nakayama, K. Roelofs, V. T. Lee, H. O. Sintim, *Mol. Biosyst.* **2012**, *8*, 726-729; e) B. Wang, Z. Wang, U. Javornik, Z. Xi, J. Plavec, *Sci. Rep.* **2017**, *7*, 16550; f) C. Wang, M. Sinn, J. Stifel, A. C. Heiler, A. Sommershof, J. S. Hartig, *J. Am. Chem. Soc.* **2017**, *139*, 16154-16160.

[17] a) P. Puig, A. Terron, V. Moreno, *Inorg. Chim. Acta* **1986**, *123*, 87-90; b) R. Cini, G. Giorgi, *Inorg. Chim. Acta* **1987**, *137*, 87-90; c) P. Zhou, R. Shi, J.-F. Yao, C.-F. Sheng, H. Li, *Coord. Chem. Rev.* **2015**, *292*, 107-143.

[18] H. Sigel, R. Griesser, *Chem. Soc. Rev.* **2005**, *34*, 875-900.

[19] B. L. Gaffney, E. Veliath, J. W. Zhao, R. A. Jones, *Org. Lett.* **2010**, *12*, 3269-3271.

[20] S. Otto, F. Bertoncin, J. Engberts, *J. Am. Chem. Soc.* **1996**, *118*, 7702-7707.

Entry for the Table of Contents

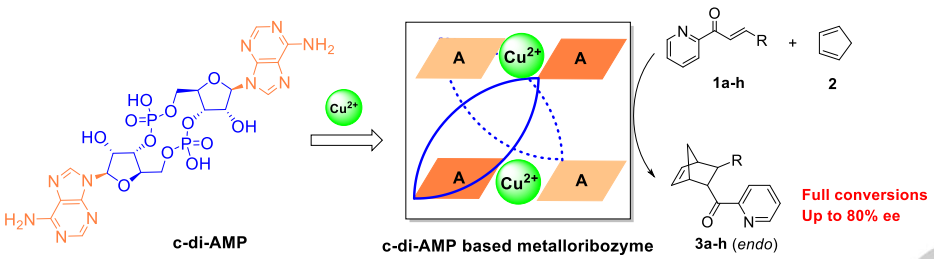

c-di-AMP based enantioselective catalysis: A small cyclic RNA of c-di-AMP and Cu^{2+} ions could assemble into an artificial metalloribozyme that is able to catalyze the enantioselective Diels–Alder reactions with up to 80% *ee*. The presence of c-di-AMP in the metalloribozyme not only achieves the chirality transfer but also gives rise to a significant rate enhancement.